Exploration of playa surface crusts in Qehan Lake, China through field investigation and wind tunnel experiments

LIU Dongwei[1], HAN Lijing[2*], KOU Zihan[1], GAO Xinyu[1], WANG Jingjing[1]

[1] School of Ecology and Environment, Inner Mongolia University, Hohhot 010021, China;
[2] College of Geography and Remote Sensing Sciences, Xinjiang University, Urumqi 830017, China

Abstract: Globally, many lakes are drying up, leaving exposed lakebeds where wind erosion releases dust and sand rich in salt and harmful heavy metals into the atmosphere. Therefore, understanding the characteristics and spatial distribution of playa surface crusts is important to recognize the manifestation of salt dust storms. The objective of this study was to explore the playa surface crust types as well as their spatial distribution and evolution of Qehan Lake in Inner Mongolia Autonomous Region, China to understand the salt dust release potential of different types of playa surface crusts. Various crust characteristics were investigated by field sampling in Qehan Lake, and playa surface crusts were further divided into five types: vegetated areas, salt crusts, clay flats, curly crusts, and margins. It should be noted that curly crusts were distributed in clay flats and covered only a small area in Qehan Lake. The spatial distribution characteristics of playa surface crust types were obtained by supervised classification of remote sensing images, and the salt dust release potential of crusts was explored by the wind tunnel experiments. The field investigation of Qehan Lake revealed that playa surface crust types had a circum-lake band distribution from the inside to the outside of this lake, which were successively vegetated areas, clay flats, salt crusts, and margins. The spatial distribution patterns of playa surface crust types were mainly controlled by the hydrodynamics of the playa, soil texture, and groundwater. There was a significant negative correlation between crust thickness and electrical conductivity. The results of the wind tunnel experiments showed that the initial threshold of friction wind velocity for the salt dust release was higher in clay flats (0.7–0.8 m/s) than in salt crusts (0.5–0.6 m/s). Moreover, the particle leap impact processes occurring under natural conditions may reduce this threshold value. Salinity was the main factor controlling the difference in the initial threshold of friction wind velocity for the salt dust release of clay flats and salt crusts. This study provides a scientific reference for understanding how salt dust is released from a lakebed, which may be used for ecological restoration of dry salt lakes.

Keywords: playa surface crust; curly crusts; salt crusts; salt dust release; wind tunnel experiments; Qehan Lake

1　Introduction

Lakes in arid and semi-arid areas have been affected by climate change and human activities in recent years, causing water bodies to dry up and lakebed to be exposed (Tao et al., 2015; Micklin, 2016; Chun et al., 2017; Zhang et al., 2019). Drying saline lakebeds (Buck et al., 2011; Goldstein

et al., 2017) further develop into playas, which are unique desert landscapes in arid and semi-arid areas (Peterson, 1980; Briere, 2000; Yechieli and Wood, 2002; Wurtsbaugh et al., 2017). Playa surfaces are often fluffy and highly vulnerable to wind erosion. During wind erosion events, dust may be transported by wind over long distance, thus affecting the ecological environment of the surrounding areas (Blank et al., 1999; Reynolds et al., 2007; Liu et al., 2011a; Zlotnik et al., 2012; White et al., 2015). Examples of this phenomenon include the Ebinur Lake in China (Liu et al., 2011b), Aral Sea in Central Asia (Micklin, 2016), Sevier Dry Lake in USA (Hahnenberger and Perry, 2015), and Lake Urmia in Iran (Mardi et al., 2018). The dust emitted by playas, consisting of a high concentration of hazardous chemicals (heavy metals, salt ions, etc.), might infiltrate human body via air circulation and negatively impact health. Therefore, clarifying the dynamics of dust emissions from playa surfaces and their influencing factors is necessary to alleviate this environmental problem.

Soil crusts can be divided into physical and biological categories on the basis of their formation mechanisms (Pagliai and Stoops, 2010). Playas are characterized by the existence of surface crusts, which vary with the weather and climate, and the morphology of playa surface crusts change with surface temperature and soil moisture over time (Nield et al., 2015, 2016a). Crusts increase as the surface dries and cracks, affecting the surface morphology (Valentin and Bresson, 1992). Playa surface crusts are sensitive to the surrounding environment and show rapid changes, especially during seasonal alternations (Nield et al., 2015). As the crusts develop, the surface aerodynamic properties change, which profoundly affects the emission of dust containing salt (salt dust hereafter). Therefore, it is necessary to quantify the surface crusts to study salt dust. Salt dust emission in playas is strongly influenced by the surface soil moisture and crust types (Reynolds et al., 2007). Both high-frequency temporal dynamic changes and spatial distribution differences in the morphology of surface crusts control the salt dust release potential (Nield et al., 2016b). The relationship between the physical and chemical characteristics of playa surface crusts, especially the type and form of salt crusts that affect the wind erosion potential of surface crusts, is rather complex (Nield et al., 2016a). Factors affecting the wind erosion resistance of surface crusts may include precipitation, temperature, soil texture, soil organic matter, salt type and structure, soil electrical conductivity (EC), and calcium carbonate equivalents (Sweeney et al., 2011; Nield et al., 2016a; Goldstein et al., 2017; Motaghi et al., 2020).

Playa surface crusts have various forms, such as smooth crusts, weak botryoidal crusts, polygon crusts, and smooth salt crusts (Chico, 1968). Crust types have yet to be thoroughly investigated because the characteristics of playa surface crusts differ across different geographical areas. A systematic classification study of playa surface crust types is necessary to better quantify the effects of crustal properties on salt dust release. Cahill et al. (1996) revealed that stable salt-silt-clay crusts can form on the surface of Owen Lake, USA; then, polygonal crusts can be formed after the degradation of the lake, and salt dust can be further generated through the saltation-abrasion process. The different playa surface crust types exhibit heterogeneity and may show differences in dust release potential. Sweeney et al. (2011) investigated the dust release from desert landscapes in the eastern Mojave Desert, USA, and found that the strongest dust release occurs at the sandy playa margins. Motaghi et al. (2020) classified playa surface crust types into four types: clay flats, clay flats-salt crusts, salt crusts, and salt crusts-clay flats. They also calculated soil erodibility fractions for comparison and revealed that salt crusts are more stable and less susceptible to erosion. Contradictory to these results, a previous study has shown that the playa with sand-salt crusts is the most unstable type and prone to salt dust storms (Alkhayer et al., 2019).

In this study, we explored the characteristics and spatial distribution of soil crust properties of playa surface crusts in Qehan Lake, Inner Mongolia Autonomous Region of China through field investigation, and determined the salt dust release potential of major crust types by the wind tunnel experiments. The main objectives are (1) to clarify the classification and spatial patterns of playa surface crusts and explain their causes; (2) to investigate which types of crusts are more prone to release salt dust; and (3) to investigate the effects of salt, water content, and soil texture

on salt dust release. The results from this study may provide scientific reference to clarify the formation and evolution of surface crusts in playas and understand the situation of salt dust release for rational planning of ecological restoration project in Qehan Lake.

2   Materials and methods

2.1   Study area

Qehan Lake (43°52′–43°58′N, 114°46′–115°02′E) is located in the southwest of the Abag Banner of Xilin Gol League, Inner Mongolia Autonomous Region of China. The lake extends from southwest to northeast, and is divided into two parts by an artificial dam, namely East Qehan Lake and West Qehan Lake (Fig. 1a). Specifically, East Qehan Lake has an area of 28.0 km^2 and a maximum water depth of 7.2 m, while West Qehan Lake has an area of 80.0 km^2 and has gradually dried up with increasingly exposed lakebed since the early 2000s. To the south of Qehan Lake is the Hunshandake Sandy Land, and to the north is the Abag Lava Plateau. The Abag Lava Plateau is rich in acid volcanic clastic rocks, sedimentary rocks, sandstone, sandy mudstone, glutenite, mudstone, and other easily eroded rocks, which are highly susceptible to leaching. Two seasonal rivers, i.e., Gogusty River and Engel River, flow into East Qehan Lake and West Qehan Lake, respectively.
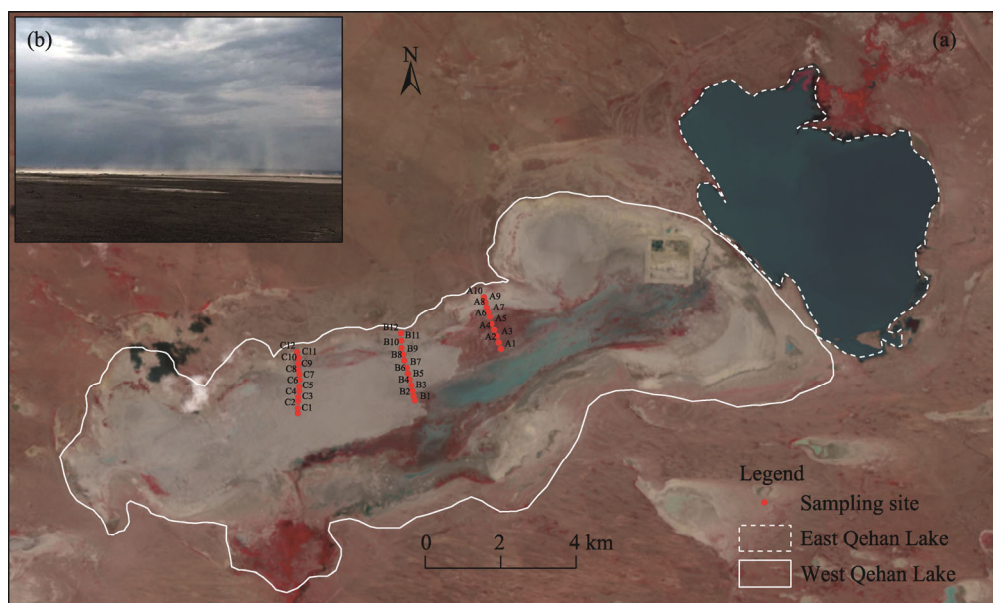
Fig. 1   Landsat image overview of Qehan Lake including East Qehan Lake and West Qehan Lake (a), and photo showing salt dust blowing over the playa (b). The Landsat-8 satellite false-color composite image (RGB bands 543) was captured on 14 July, 2019.

Influenced by the Siberian highlands, the area has a temperate continental climate characterized by cold, dry, and windy. The average annual precipitation is about 280 mm, with about 70% of precipitation occurring from June to August. Seasonal waterlogging depends mainly on rainfall (Chun et al., 2017). Since the area is generally dry, potential evaporation is much greater than precipitation. Frequent windy weather, with wind speeds up to 15.0 m/s, affects the playa surface as it is highly vulnerable to wind erosion. Blowing salt dust often occurs over the playa surface (Fig. 1b). To solve this problem, *Suaeda glauca* was planted locally for ecological restoration and salt dust prevention. Salt dust is often captured in areas with normalized difference vegetation index (NDVI) values below 0.25, but this range is difficult to demarcate.

chinaXiv:202305.00136v1

2.2   Soil sampling and processing

Measurement sites were marked along the belt transects A (sites A1–A10), B (sites B1–B12), and C (sites C1–C12) (Fig. 1), with a total of 34 sampling sites. The geographical coordinates of each sampling site were recorded using a portable GPS (G120, UniStrong, Beijing, China) with an accuracy of 3.0 m. During the field sampling, we found that the distribution of crusts from the lakebed center to the lakeshore showed a zonal distribution, which is conducive to the investigation of the regularity of crusts. Moreover, since no precipitation occurred during the sampling period, crusts did not change quickly enough to cause a change in playa surface crust type. Soil crust thickness and crust hardness were measured on topsoil (0.00–10.00 cm) at each site using a vernier caliper with the precision of ±0.03 mm (DL91300, Deli Group, Ningbo, China) and a pocket soil penetrometer (16-T0171, Zhuozhou Tianpeng, Baoding, China), respectively, and measurements were repeated 10 times for each sampling site with an area of approximately 1.0 m^2 on 7 and 8 July, 2019. Vertical downward pressure was applied to the pocket soil penetrometer at the sampling site to obtain a reading when soil crust was broken. After that, one soil sample was collected at each sampling site using a soil auger, and a total of 34 soil samples were collected to measure soil water content, EC$_{1:5}$ (the electrical conductivity of the upper clear layer for a soil-to-water ratio of 1:5), and soil particle size.

Soil water content was determined using the oven-drying method in the laboratory of the School of Ecology and Environment, Inner Mongolia University, Hohhot, China. Soil samples were air-dried in the laboratory for EC$_{1:5}$ analysis. Specifically, the air-dried soil samples were passed through a 2 mm sieve, of which approximately 50 g soil was placed into a conical flask containing 250 mL of deionized water, then the flask was shaken mechanically for 30 min until soil salts were completely dissolved. After 24 h of resting, the supernatant was filtered using qualitative filter papers. The filtrated clear liquid was controlled at 25°C, and EC$_{1:5}$ was measured using a portable conductivity meter (Multi 3420, WTW, Weilheim, Germany). After natural air drying, 5 g of soil was added to the beaker and 10% H$_2$O$_2$ was added for heating reaction to remove organic matter, then 10% HCL was added for heating reaction to remove carbonate. Additionally, 100 mL of deionized water was added and the supernatant was extracted after standing for 24 h. Finally, 2% Sodium (hexa) meta phosphate was added as dispersant, and soil particle composition was measured by a particle size analyzer (S3500, Microtrac MRB, Montgomeryville, USA) after shock.

To investigate the effects of different playa surface crust types on salt dust release, we set five salinity class gradients for *in situ* soil sample collection using a soil three-parameter sensor (WET-2, Delta-T Devices, Cambridge, England) with three replicates per sampling site, resulting in a total of 15 soil samples for each site. *In situ* soil samples were collected in rectangular wooden boxes (50.00 cm×30.00 cm×10.00 cm), encapsulated in wooden boards, and wrapped in cling film and plastic on the outermost layer to reduce water evaporation. After encapsulation, the boxes were taken to the wind tunnel laboratory of Lanzhou University, Lanzhou, China, for further experiments.

2.3   Classification and mapping of playa surface crust types

Combined with previous taxonomic studies on playa surface crusts, the classification of the physical properties of soil crusts may effectively explain the impacts of playa surface crusts on salt dust release and help to identify the types of crusts that are more likely to release salt dust (Krinsley, 1970; Sweeney et al., 2011; Motaghi et al., 2020). According to Krinsley (1970), the classification method of playa surface crusts can categorize crust types based on sediment surface features. Motaghi et al. (2020) also used this classification system and spatially mapped the playa surface crust types of Lake Urmia in Iran with Landsat satellite image data and supervised classification algorithms. Thus, playa surface crusts in the study area can be classified and mapped using Sentinel-2 satellite images and supervised classification methods to clarify their spatial distribution characteristics. The Sentinel-2 satellite images (mosaic function synthetic images from 1 to 31 July in 2019) were obtained from Google Earth Engine (https://earthengine.google.com/), then classified and mapped with reference to the location

information of the sampling sites. We classified the playa surface crusts into salt crusts, clay flats, vegetated areas, curly crusts, and margins based on salt precipitation deposits, vegetation, compacted clays, and gravels (Krinsley, 1970; Sweeney et al., 2011; Motaghi et al., 2020). Due to the small size (<100.0 m^2) and fragmentation of curly crusts, their geographical distribution could not be clearly seen using satellite images.

2.4 Wind tunnel experiments

The salt dust release experiments were conducted in the wind tunnel laboratory of Lanzhou University, and the schematic diagram of the wind tunnel experiment is shown in Figure 2. The detailed structure of the wind tunnel was described by Zhang et al. (2014). In order to simulate the real playa surface, we placed an artificial turf (length of 80.00 cm, width of 120.00 cm, and thickness of 1.00 cm) in front of soil samples in the wind tunnel experiments. A groove (length of 50.00 cm and width of 30.00 cm) was constructed at the downwind axis of the wind tunnel section to facilitate the placement of the soil sample box. The upper surface of the soil sample box was flushed with the wind tunnel surface to ensure the accuracy of the experimental data, which is similar to the treatment described by Nield et al. (2016a). A sand collector was placed 20.00 cm behind the central axis of the soil sample box to measure the horizontal dust flux; the collector consists of 14 rectangular sand collection ports (length of 4.00 cm and height of 1.50 cm) distributed along the vertical direction. The end of the sand collector was oriented downwards at an angle of 30° to the horizontal dust flux to better collect soil particles into the bottom of the sand collector by gravity. The sand collector was weighed at the end of each wind tunnel experiment, and the horizontal dust flux was calculated. The wind tunnel rotors started at 6000 r/min and increased by 1000 r/min during each experiment for 180 s until the sand collector started to collect salt dust, and the sand collector was weighed before the speed was increased. The soil samples in the wind tunnel experiments were divided into five groups (I, II, III, IV, and V, with the mean EC$_{1:5}$ values of 10.85, 7.21, 3.37, 2.30, and 8.70 mS/cm, respectively) and the measurements were replicated three times for each soil sample. The wind velocity observed through the pitot tube can be converted into friction wind velocity (u^*; m/s) using the logarithmic law of Prandtl-Karman (Prandtl, 1935):

$$u(z) = \frac{u^*}{k} \ln\left(\frac{z}{z_0}\right),$$ (1)

where $u(z)$ (m/s) is the wind velocity at height z (m) above the surface; k is the dimensionless von-Kármán constant with a universal value of 0.40; and z_0 (m) is the surface aerodynamic roughness.
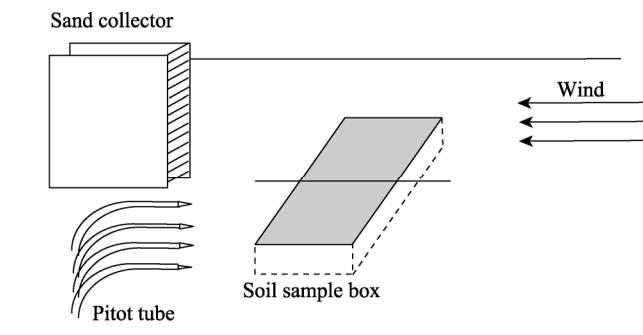

Fig. 2 Schematic diagram of the wind tunnel experiment

2.5 Statistical analysis

Pearson correlation coefficient was calculated using SPSS Statistics 26 (IBM, New York, USA), which was used to analyze the correlations among soil water content, EC$_{1:5}$, crust hardness, and crust thickness. The bar graphs, box line plots, and scatter plots were illustrated using Origin 2022

(OriginLab, Northampton, Massachusetts, USA). The spatial distribution of playa surface crust types was plotted by ArcMap 10.8 (Esri, Redlands, USA).

3　Results

3.1　Classification and characterization of playa surface crust types

Figure 3 and Table 1 show the classification and characterization of playa surface crust types in the study area according to previous studies (Krinsley, 1970; Sweeney et al., 2011; Schoeneberger et al., 2012; Motaghi et al., 2020).
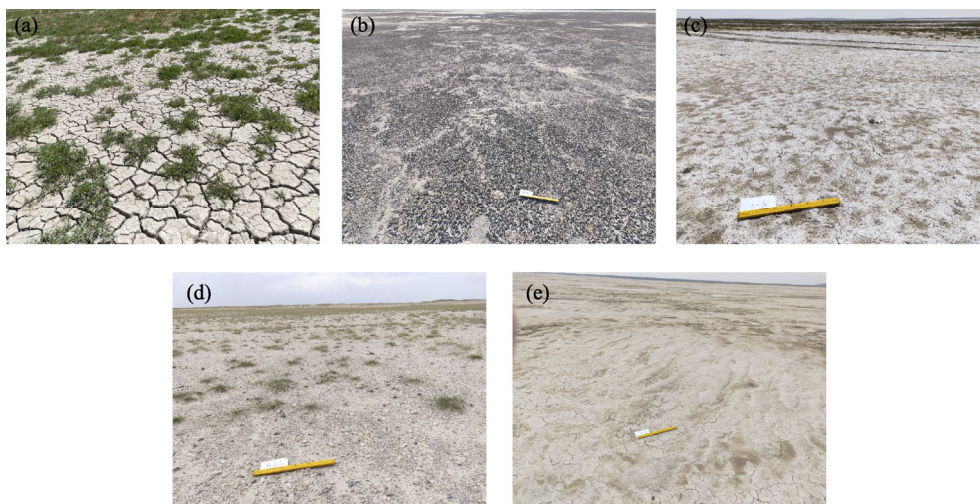
Fig. 3　Field images used for classifying playa surface crust types of the sampling sites. (a), vegetated areas located close to the center of the lake; (b), curly crusts occurred in a clay flat with a small area; (c), salt crusts located between the edge of the playa surface and clay flats; (d), margins appeared on the lakeshore; (e), clay flats occurred between vegetated areas and salt crusts.

Table 1　Description of playa surface crust types in Qehan Lake

| Playa surface crust type	Crust kind	Crack kind	Description
Vegetated areas	Physical	RCR, ICR, and RTH	Large cracks with width higher than 1.00 cm and depth greater than 3.00 cm (trans-horizon). Crusts appear polygonal in shape, with large polygons accompanied by crust-related cracks inside. They are seasonal, formed by wetting and drying of the soil. The dominate plant species is *Suaeda glauca*.
Salt crusts	Physical and chemical	RCR	Cracks with width less than 0.50 cm and depth of 0.50 cm. The surface soil is swell and saline.
Clay flats	Physical	RCR	Shallow and transient (generally persist less than a few weeks) RCR at some locations. There are signs of salt dust release and wind erosion (Fig. 1b).
Curly crusts	Physical	RCR	Brittle curly crusts. The area is very small and highly susceptible to wind erosion.
Margins	Physical	None	There is coarse and fine gravel, sand, and lakeside vegetation (*Achnatherum splendens*, *Nitraria tangutorum*, and *Stipa capillata*).

Note: RCR, reversible crust-related cracks; ICR, irreversible crust-related cracks; RTH, reversible trans-horizon cracks.

The results indicated that the study area included five playa crust types: vegetated areas, salt crusts, clay flats, curly crusts, and margins. Compared to clay flats, the wider and deeper crustal cracks distributed in vegetated areas may be caused by the higher silt particle content in vegetated areas than in clay flats. Large cracks crossed two vertical horizons (trans-horizon cracks) on the surface of salt flats in vegetated areas, showing the cracked crust with a depth greater than 3.00 cm overlying a compact unfractured silt deposit. The cracks themselves were mostly distributed nonlinear, indicating many dry-wet cycles, and the intersection of cracks is irregular (Tang et al.,

2008; Goehring et al., 2010; Goehring, 2013). The growth of vegetation in vegetated areas may be attributed to the shallow water table, which is conductive to plant growth. Salt crusts, clay flats, and curly crusts were all reversible crust-related cracks, while vegetated areas were relatively more complex. The surface of salt crusts was smooth and enlarged, with salt crystal powder precipitating from evaporated salt around small cracks. The concave-up curling was the main feature of curly crusts that preferentially occurred around the perimeter of low-lying areas subject to microtopography, sometimes accompanied by ponding water. Margins were located at the edge of playa surface, and the sparse vegetation cover was insufficient to suppress the salt dust phenomenon when strong winds occurred.

3.2   Classification statistics of playa surface crust types

Figure 4 shows the differences in crust thickness, crust hardness, soil water content, and $EC_{1:5}$ for each playa surface crust type. The results indicated that the crust thickness of vegetated areas, salt crusts, clay flats, and curly crusts mainly ranged between 0.50 and 0.70 cm, with higher values up to 1.00 cm or even larger in vegetated areas and salt crusts. In terms of crust hardness, salt crusts had the widest range of $0.30 \times 10^5 – 8.53 \times 10^5$ N/m². Vegetated areas had the greatest crust hardness value, while no significant difference in hardness was observed between clay flats and curly crusts. Curly crusts had similar hardness to other playa surface crust types that had been
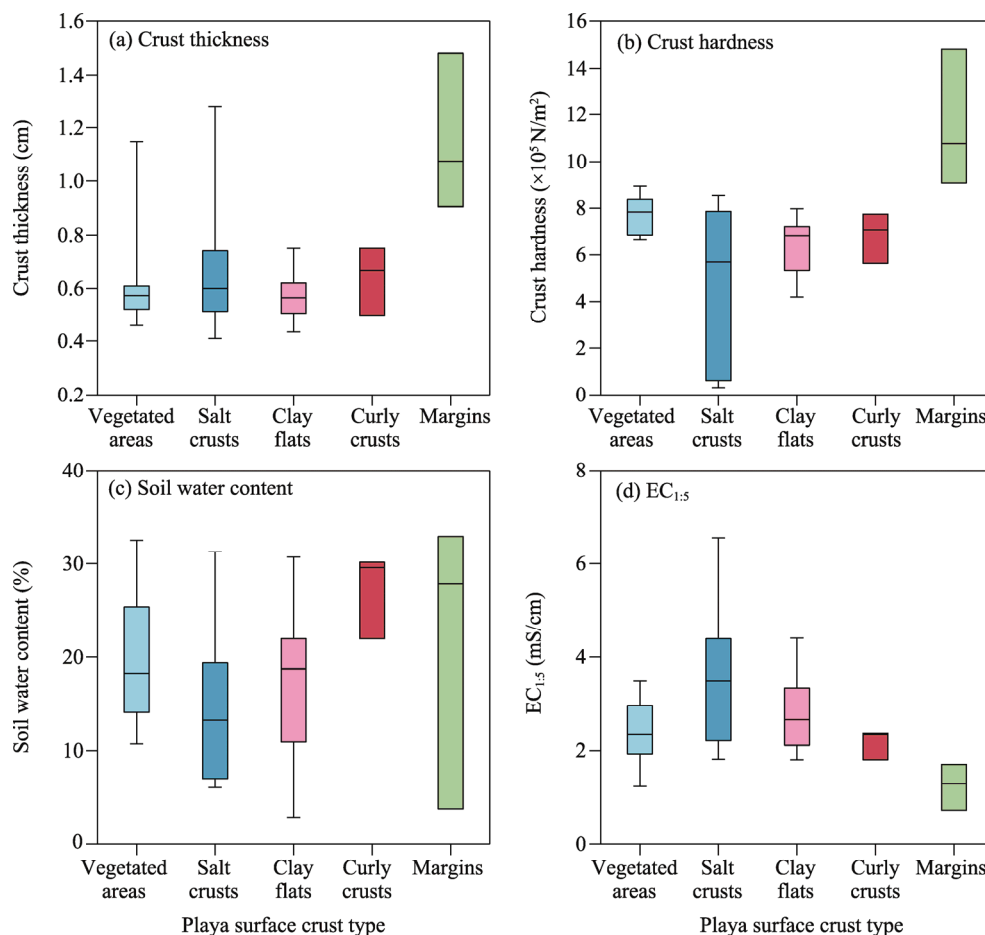
Fig. 4   Box plot statistics of crust thickness (a), crust hardness (b), soil water content (c), and $EC_{1:5}$ (electrical conductivity of the upper clear layer for a soil-to-water ratio of 1:5; d) of different crust types on the playa surface in Qehan Lake. The upper and lower limits of the box indicate the 75th and 25th percentile values, respectively; the horizontal line in each box represents the median of the distributions; and the upper and lower whiskers show the 95th and 5th percentile values, respectively.

transformed by minerals into a horizontal "mat" or a small polygonal plate. Regarding soil water content, four types were distributed from dry to wet (salt crusts, clay flats, curly crusts, and vegetated areas), with salt crusts and clay flats having lower moisture overall. The order of $EC_{1:5}$ from high to low was as follows: salt crusts, clay flats, curly crusts, and vegetated areas. Salt crystals in salt crusts were the main source of EC in the topsoil. The $EC_{1:5}$ of vegetated areas ranged from 1.00 to 3.50 mS/cm, indicating suitability for the growth of *Suaeda glauca*. The correlation results shown in Table 2 indicated a significant negative correlation between crust thickness and $EC_{1:5}$ of the topsoil. The salt in the playa topsoil expanded the surface layer while decreased the thickness of playa surface crusts, forming a thin, brittle crust containing salt sediments. This suggests that salt may be one of the main factors influencing the thickness of surface crusts in Qehan Lake.

Table 2   Pearson correlation results of crust thickness, crust hardness, soil water content (topsoil), and $EC_{1:5}$

	Crust thickness	Crust hardness	Soil water content	$EC_{1:5}$
Crust thickness	1.000			
Crust hardness	0.181	1.000		
Soil water content	0.095	−0.275	1.000	
$EC_{1:5}$	−0.453**	−0.266	0.059	1.000

Note: $EC_{1:5}$ is the electrical conductivity of the upper clear layer for a soil-to-water ratio of 1:5. **, significant at $P<0.01$ level.

3.3   Spatial distribution of playa surface crust types

Figure 5 shows the results of the spatial distribution of playa surface crust types in Qehan Lake. A certain regularity was observed in the spatial distribution of playa surface crust types, which can be summarized as vegetated areas, clay flats, salt crusts, and margins from the lake center to the lakeshore. Curly crusts were not demonstrated because of small area and rarity in playa surface.
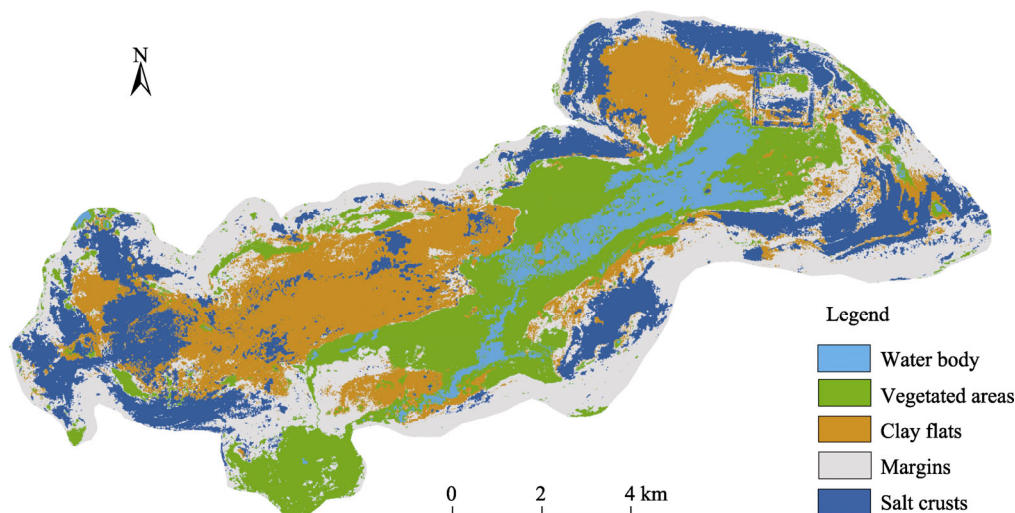

**Fig. 5**   Spatial distribution of playa surface crust types in Qehan Lake

Figures 6 and 7 indicate the variations of crust thickness and hardness from the lake center to the lakeshore for the three belt transects (A, B, and C). Crust thickness showed no significant variation from the lake center to the lakeshore along the belt transects A (except for A7), B, and C, and crust thickness was essentially the same but larger near the lakeshore (B11, B12, C11, and C12), as shown in Figure 6. Crust thickness tended to increase from the lake center to the lakeshore and was more pronounced along the belt transect C. Differences in crust thickness were primarily found at sampling sites located near the lakeshore (e.g., B11, B12, C11, and C12), which were mainly covered by smooth alluvium and large gravels. Crust thickness at these sites

was relatively larger, ranging from 0.80 to 1.80 cm. A curly, thin crust was observed at site B4. For crust hardness, it showed little change from the lake center to the lakeshore, as shown in Figure 7. Therefore, we concluded that crust thickness was relatively uniform at the sampling sites located in the lake basin but crust hardness differed among the sampling sites, similar to the results shown in Figure 4.
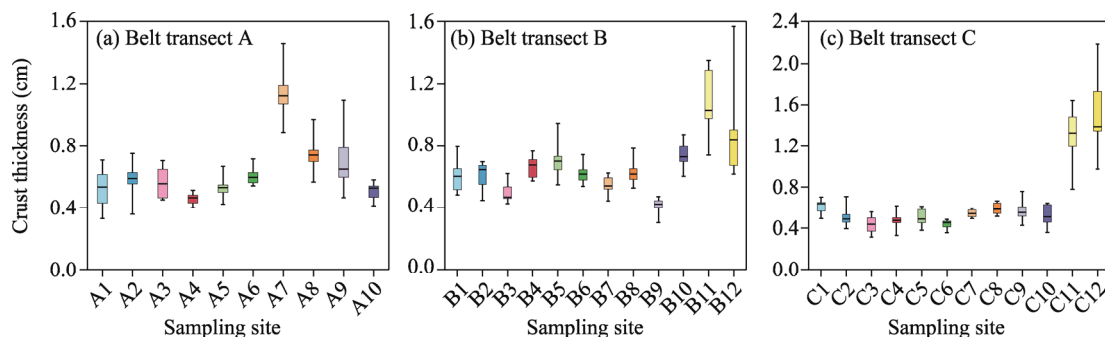
Fig. 6 Box plots of crust thickness for each sampling site from the lake center to the lakeshore in belt transects A (a), B (b), and C (c). The upper and lower limits of the box indicate the 75th and 25th percentile values, respectively; the horizontal line in each box represents the median of the distributions; and the upper and lower whiskers show the 95th and 5th percentile values, respectively.
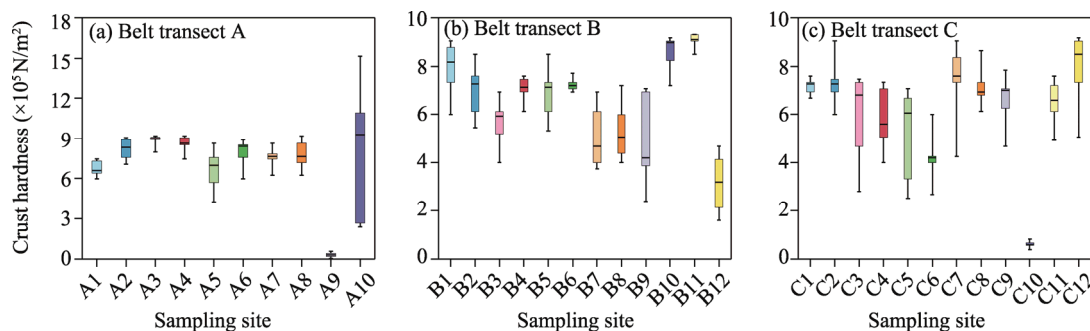

Fig. 7 Box plots of crust hardness for each sampling site from the lake center to the lakeshore in belt transects A (a), B (b), and C (c). The upper and lower limits of the box indicate the 75th and 25th percentile values, respectively; the horizontal line in each box represents the median of the distributions; and the upper and lower whiskers show the 95th and 5th percentile values, respectively.

### 3.4 Relationship between crust thickness and hardness

As shown in Figure 8, there existed a weak relationship between crust thickness and hardness. Crust hardness at sampling sites mainly ranged from 4.19×10^5 to 8.91×10^5 N/m^2, although the hardness at A9, B12, and C10 was below 2.35×10^5 N/m^2. The playa surface crust type of A9 and C10 was classified as salt crusts, and the salt crust expansion might have contributed to its low hardness. Site B12 was classified as margins, located on the lakeshore with smaller hardness due to the sandy soil. In terms of thickness, the crust thickness of most sampling sites ranged between 0.40 and 0.90 cm, while crust thickness at sampling sites A7, B11, C11, and C12 was larger than 1.00 cm. Sampling site A7 was identified as clay flats, and sites B11, C11, and C12 were margins. Without considering outliers, crust thickness showed a linear relationship with crust hardness.

3.5 Characteristics of soil samples for the wind tunnel experiments

$EC_{1:5}$, crust thickness, and soil water content of the five soil sample groups (I, II, III, IV, and V) were measured in the wind tunnel experiments (Fig. 9). Crust thickness was the highest in group III, while difference in crust thickness was little for the other four groups. Soil water content also showed a good gradient variation from high to low in the order of II, I, IV, V, and III. Specifically, soil water content was the lowest for group III, and the difference within the group was not significant, mainly because of its high sand content and poor water retention capacity.
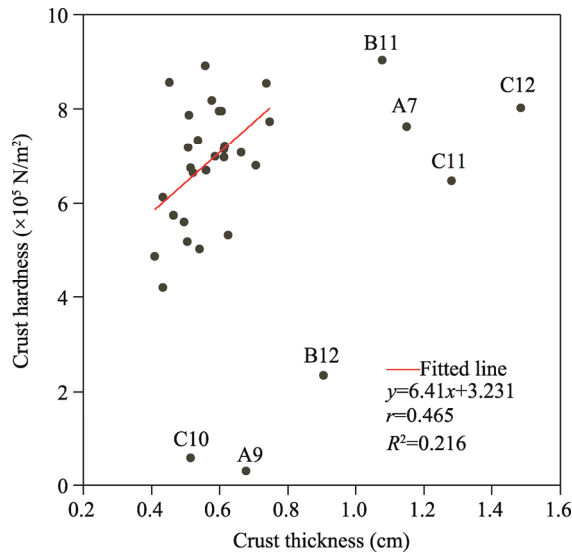
Fig. 8 Scatter plot of crust thickness and hardness. Outlier sampling sites are marked in the figure. The red line indicates the fitted line after removing the outliers with the equation statistics in the lower right corner.
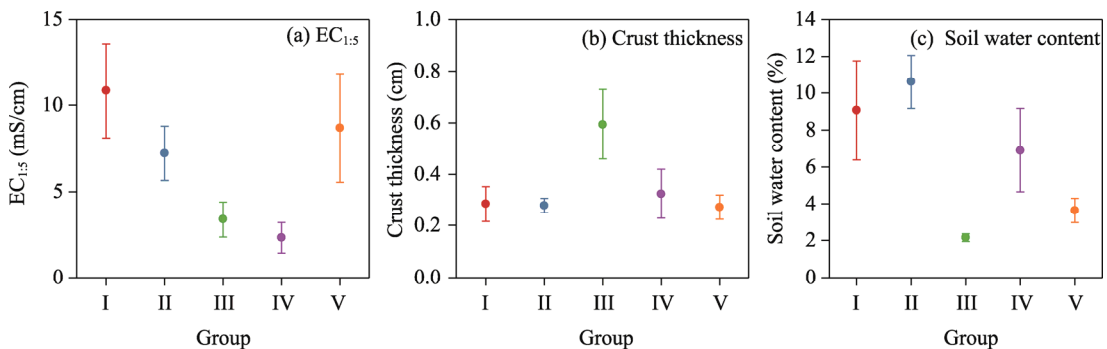
Fig. 9 Means and standard deviations of $EC_{1:5}$ (a), crust thickness (b), and soil water content (c) for the five soil sample groups (I–V) from the wind tunnel experiments. The circles indicate the means and the bars indicate the standard deviations.

The physical properties of soil samples used in the wind tunnel experiments are shown in Table 3. There was a good variety of soil samples in different groups based on sand or silt particle size. Sand particles of the five groups were sorted in ascending order as I, IV, II, V, and III, while silt particles were sorted in descending order as I, IV, II, V, and III. The soil texture category contained four types: silty loam (I1, I2, and I3), sandy loam (II2, IV1, IV2, and IV3), loamy sand (II1, II3, III1, V2, and V3), and sand (III2, III3, and V1), among which 1, 2, and 3 represent the number of repeated samples in the wind tunnel experiments. The low silt and clay content of soil samples from clay flats used in the wind tunnel experiments might be because the samples used for particle size testing were collected at the end of the wind tunnel experiments, resulting in a relatively increase in the size of the fine particles blown away from surface crusts. The particle size distribution of clay flats from other sampling sites (Fig. S1) indicated that the soil texture of clay flats was silt with particle sizes ranging from 2 and 50 µm.
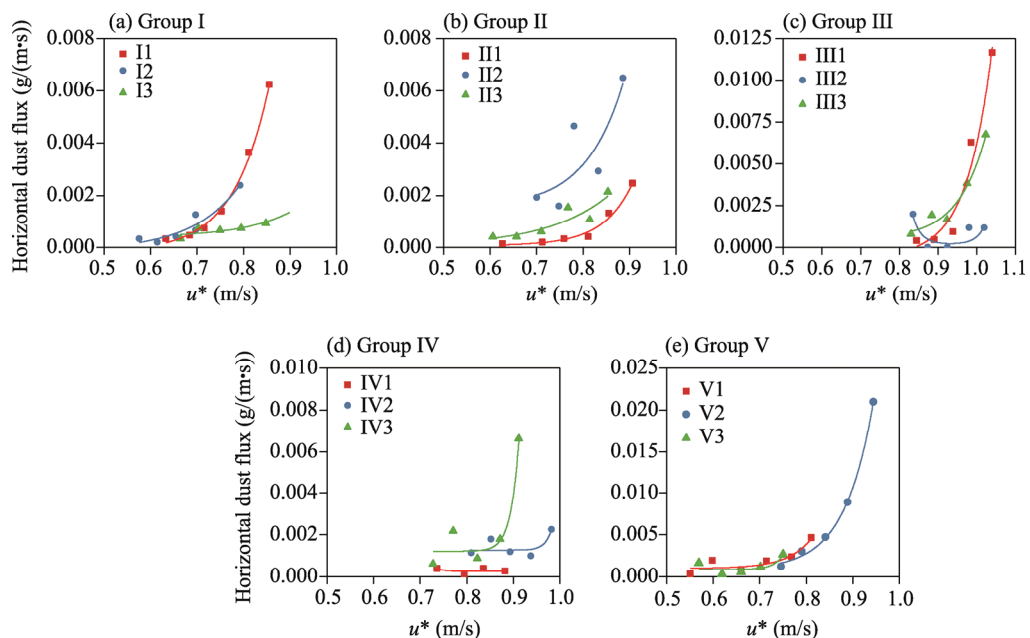
3.6 Horizontal dust flux

Figure 10 shows the variation in the horizontal dust flux with u^* calculated from the sand collectors in the wind tunnel experiments. The horizontal dust flux of each soil group exhibited an exponential relationship with u^*. The horizontal dust flux corresponding to the lowest u^* was indicative of the wind erosion resistance of soil samples. During the wind tunnel experiments, soil

Table 3 Properties of soil samples used in the wind tunnel experiments and corresponding playa surface crust types

Group	No.	$EC_{1:5}$ (mS/cm)	Crust thickness (cm)	Soil water content (%)	Sand (%)	Silt (%)	Clay (%)	Soil texture	Playa surface crust type
I	I1	13.83	0.29	7.30	41.13	58.04	0.83	Silty loam	
	I2	7.26	0.37	10.80	25.55	72.09	2.36	Silty loam	Salt crusts
	I3	11.46	0.20	4.30	33.92	59.75	6.33	Silty loam	
II	II1	7.07	0.29	9.30	76.11	22.77	1.12	Loamy sand	
	II2	9.22	0.24	11.10	67.94	32.06	0.00	Sandy loam	Salt crusts
	II3	5.35	0.30	9.20	70.76	28.86	0.38	Loamy sand	
III	III1	4.42	0.78	1.80	84.42	14.52	1.06	Loamy sand	
	III2	3.70	0.51	2.40	89.68	9.73	0.59	Sand	Clay flats
	III3	1.98	0.49	2.30	91.85	7.66	0.49	Sand	
IV	IV1	2.13	0.34	10.50	64.33	35.67	0.00	Sandy loam	
	IV2	1.32	0.43	7.40	72.48	24.90	2.62	Sandy loam	Clay flats
	IV3	3.44	0.20	7.70	63.54	35.68	0.78	Sandy loam	
V	V1	4.45	0.34	4.16	91.07	8.93	0.00	Sand	
	V2	12.00	0.23	3.55	76.94	23.06	0.00	Loamy sand	Salt crusts
	V3	9.66	0.25	4.56	83.44	16.56	0.00	Loamy sand	

Note: The values 1, 2, and 3 after I–V represent the number of repeated samples in the wind tunnel experiments.

Fig. 10 Relationship between horizontal dust flux and friction wind velocity (u^*) for the five soil groups in the wind tunnel experiments. (a), group I; (b), group II; (c), group III; (d), group IV; (e), group V. The values 1, 2, and 3 after I–V represent the number of repeated samples in the wind tunnel experiments. The lines are the fitted lines of horizontal dust flux against u^*.

particles can be captured at u^* of 0.6 m/s for groups I, II, and V, while for groups III and IV, soil particles can be collected at u^* of 0.7 m/s. This indicated that crust-type clay flats (groups III and IV) had higher wind erosion resistance than salt crusts (groups I, II, and V). It is worth noting that for groups III2 and V3, after initial salt dust releasing, the horizontal dust flux decreased first and

then increased exponentially, while groups II2 and IV3 showed a sudden increase in the horizontal dust flux, both of which may be related to the instantaneous destruction of soil crusts.

4   Discussion

4.1   Spatial patterns and evolution of playa surface crusts in Qehan Lake

Studying the taxonomy of lakebed (dry) crusts in different regions can help us to understand the mechanisms of crust formation. In this study, playa surface crust types in dried Qehan Lake were classified into vegetated areas, salt crusts, clay flats, curly crusts, and margins. The surface type of West Qehan Lake showed a regular pattern from the lakeshore to the lake center, with the outer margins surrounding the playa. This regular distribution pattern was also reflected in soil texture, that is, margins contained more coarse sands and gravels than the central area. This indicates that hydrological processes would be the leading cause of sediment siltation. The formation of margins is mainly dominated by surface runoff, resulting in a coarser soil texture at the surrounding zones away from the lake center, including sediments and gravels brought by runoff (Sweeney et al., 2011). When sediments are deposited into the playa due to water erosion, coarse sands with large gravels are deposited before fine particles (Luo et al., 1999). The higher crust hardness of margins may be due to the fact that the gravels are filled with silt particles, which act as cement, forming a concrete-like structure that increases crust hardness. The lack of interaction with groundwater and the coarse soil texture in this area result in poor water retention, further leading to low water content in the surface soil.

In Qehan Lake, salt crusts were mainly found in regions between playa margins and clay flats or vegetated areas, which were similar to the results of Gutiérrez-Elorza et al. (2005) for the playa in the central-southern sector of the Duero Depression in Spain. It is generally accepted that the source of soil salinity is related to groundwater, and the salt is deposited on the surface by capillary forces and intense evaporation (Hassani et al., 2021). The hydrodynamics of the lakeshore are likely the reason for the salt crusts close to playa margins and the small area of the lake center. During precipitation events, surface water flows from the lakeshore into the lake center, but the flat lakebed cannot sustain the responsive dynamics. The flowing water that erodes the lakeshore and external soil containing soluble salts infiltrates the bottom near the lakeshore as it cannot continue to flow towards the lake center, resulting in the formation of salt crusts by raising the shallow water table in the zone between playa margins and vegetated areas (Luo et al., 1999; Zlotnik et al., 2012). The salt crusts of Qehan Lake mainly consist of soda salts, which are susceptible to deliquescence and moisture absorption, leading to a highly moist surface (Xisarula, 2011). The high level of sodium ions reduces the soil particle binding, and the fine-grained soil expands and disperses. This causes the salt analysis to show heterogeneity, making the range of hardness of salt crusts greater than that of other playa surface crust types. The surface crust of playa formed by the drying up of extremely saline salt lakes may contain more salts, forming hard salt crusts with resistance to wind erosion (Nield et al., 2016a; Motaghi et al., 2020). There are two possible reasons for the significant negative correlation between crust thickness and $EC_{1:5}$ (salinity) in this study. First, soda salts lead to fluffy soil and reduce crust thickness; and second, the salt content is not enough to form a pure thick salt crust, but it is still higher compared to other playa surface crust types.

Vegetated areas were near the lake center (i.e., far from the lakeshore) and dominated by silty loamy soils, where fine soil particles tend to form reversible trans-horizon cracks under strong evaporation. Vegetated areas grown with *Suaeda glauca* can inhibit the production of salt dust release (Zhao et al., 2011). In this study, vegetated areas had a dense growth of *Suaeda glauca* with root soils characterized by large mud cracks, which differed from other playa surface crust types, suggesting that vegetation growth may contribute to the formation of large mud cracks. Large cracks in vegetated areas can facilitate the preservation of alkali poncho seeds without being blown away, while reversible crust-related cracks in other playa surface crust types are less

capable of preserving vegetation seeds.

The smooth surface of clay flats is sometimes accompanied by reversible crust-related cracks, although the available groundwater table is deeper than 2.0 m. Therefore, the formation of crusts may ignore the influence of groundwater-soluble salts and mainly consider soil texture and evaporation conditions. Clay flats of Qehan Lake are mainly composed of sandy and silty loam involved in the formation process, similar to many other playas in the world (Sweeney et al., 2011; Sweeney et al., 2016; Goldstein et al., 2017; Motaghi et al., 2020).

Curly crusts mainly appeared in the low-lying area of the lake basin and had a relatively high humidity. A thin and high silt-content sedimentary layer temporarily formed at the bottom of the turbid puddle, and the thin layer curled after rapid dehydration. The concave-up curling might be explained by the non-uniform distribution of horizontal forces generated by the development of capillary forces (Tran et al., 2019). Mud curls are fragile and easily broken, thus providing the base materials for salt dust transport (Stout, 2007).

4.2   Sand dust release from different playa surface crust types

Generally, sand-sized sediments occurring in dry lakebeds are supplied by adjacent dunes or post-flood deposits that release salt dust from compacted clay or silt into the atmosphere and produce additional fine particles through leapfrog impact and creep abrasion processes (Gomes et al., 1990; Stout, 2003). Cahill et al. (1996) focused on crusted playa surfaces, regions of loose and coarse detrital particles (sand and dunes) in Owen (dry) Lake, USA, where salt dust was observed. Similarly, these areas existed in Qehan Lake we studied. Coarse detrital particles appeared in the area near the lake center along belt transect C that lacks vegetation and is easily exposed to salt dust release. These coarse detrital particles were located at the junction of the lakebed and lakeshore in Qehan Lake. Sand-bearing sediments released salt dust from consolidated or compacted clay and/or silt into the atmosphere. These coarse detrital particles can cause the discharge of fine dust particles from the lakebed and generate more fine dust by wind and sand abrasion. Nearby sand sources or the deposition of fine sand after floods might also supply coarse detrital particles to the bottom of ephemeral lakes (Bullard et al., 2020).

The results of the wind tunnel experiments indicated that salt dust release from clay flats could only occur at higher u^*. In nature, salt dust release may be mainly caused by human activities that destabilize the surface structure or salt dust impact (Gill, 1996; Houser and Nickling, 2001; Reynolds et al., 2007). The impact of jumping sand grains on playa surface crusts can disintegrate fine or clay-sized particles from the surface (Gillett, 1979) or the sand grains of saltation itself (Krinsley and Doornkamp, 1973). The wind tunnel experiments conducted by Zhang et al. (2016) also showed that surface renewal through saltation and soil creep is important in limiting salt dust supply. However, in this study, the wind tunnel experimental conditions lacked the process of sand grain leap, which may increase the initial threshold of u^* for the salt dust release. The results from our wind tunnel experiments showed threshold of about 0.7–0.8 m/s for salt dust release occurring on clay flats, higher than that for salt dust release occurring on salt crusts (0.5–0.6 m/s). Similar results were observed by Sweeney et al. (2011) at the playa site in the Mojave Desert, which was interpreted as clay flat crusts with higher particle cohesion. However, the study of Motaghi et al. (2020) in Lake Urmia in Iran showed that the presence of a thin layer of crystalline halite on the salt crust surface, along with permanent shallow surface water and increased soil clay content, makes this crust type more stable and resistant to wind erosion than other playa surface crust types. Although salt crusts have an inhibitory effect on salt dust release, they become more fragile and more likely to broke under continuous drought conditions and increasing aerosol concentrations (Borlina and Rennó, 2017). In addition to the protective mechanism of salt crusts, the thicker crusts of clay flats may also play a role in inhibiting salt dust release. The thick crusts formed by clay soil particles indicate a stronger aggregation of soil particles, suggesting that the salt dust release process in clay flats is mainly influenced by the impact of leaping particles. In the wind tunnel experiments, large sand particle-containing clay flats produced thick crusts that were more stable (higher u^*) than salt crusts. This may be explained by the fact that the

stability of crusts is increased by a prolonged dry period, while the particle size may indirectly impact crust thickness. The soil water content of the wet soil layer limits salt dust release at a very low level since the release of salt dust increases after evaporation, so soil thickness becomes the main limiting factor; however, both will be dominated by saltation episodes and soil agglomerate fragmentation (Huang and Gu, 2009; Dun, 2019). Our results indicated that clay flats are more prevalent when fine dust is produced by particle abrasion, and heavy pulverization of particles is released from the crust surface. Therefore, under natural conditions, the threshold value of $u*$ for salt dust release may be lower than that in the wind tunnel experiments. We found that the initiation threshold value of $u*$ for the salt dust release in Qehan Lake was higher than the threshold (0.2–0.6 m/s) reported by Nield et al. (2016a) for soil samples taken from the Botswana Sua Pan in a wind tunnel laboratory at Trent University, Canada. A possible reason for this was the use of sand collectors in this study, which could not capture fine particles such as PM10. However, our results are consistent with those of Sweeney et al. (2016), who demonstrated the threshold value of $u*$ in the range from 0.4 to 0.9 m/s and emission fluxes lower than 0.05 g/(m·s) for salt dust emission measurements, using the portable in-situ wind erosion laboratory (PI-SWERL) during the drought period in the Yellow Lake Playa of West Texas, USA.

5 Conclusions

Through a field survey of Qehan Lake in Inner Mongolia of China, we discovered that playa surface crust types could be classified into five types (vegetated areas, clay flats, salt crusts, curly crusts, and margins), which showed a belt-like distribution around the lake. The order from the outside to the inside of the lake was margins, salt crusts, clay flats, and vegetated areas, while curly crusts were distributed in small areas in clay flats. This regular spatial distribution pattern was mainly controlled by the hydrodynamics of the playa, soil texture, and shallow groundwater. Crust thickness tended to increase from the lake center to the lakeshore and it was more pronounced along the belt transect C. The results also showed that crust thickness showed a linear relationship with crust hardness without considering outliers. Therefore, crust thickness and hardness were good indicators for the classification of playa surface crust types in the study area.

A significant negative correlation was observed between crust thickness and $EC_{1:5}$. The wind tunnel experiments showed that the initiation threshold of friction wind velocity ($u*$) for the salt dust release was higher in clay flats (0.7–0.8 m/s) than in salt crusts (0.5–0.6 m/s). Thick crusts created by clay flats containing larger sand particles were more stable than those created by salt crusts. Salinity was the main factor controlling the difference in initiation threshold of $u*$ for the salt dust release between clay flats and salt crusts.

The main limitation of this study is that experiments were only conducted in wind tunnels rather than under natural conditions. Although we simulated outdoor and indoor conditions as much as possible when designing the experiments, the use of convenient on-site dust emission measurement systems (e.g., PI-SWERL) is recommended in the future studies.

Acknowledgements

References

Alkhayer M, Eghbal M K, Hamzehpour N. 2019. Geomorphic surfaces of eastern Lake Urmia playa and their influence on dust storms. Journal of Applied Sciences & Environmental Management, 23(8): 1511–1520.

Blank R R, Young J A, Allen F L. 1999. Aeolian dust in a saline playa environment, Nevada, U.S.A. Journal of Arid Environments, 41(4): 365–381.

Borlina C S, Rennó N O. 2017. The impact of a severe drought on dust lifting in California's Owens Lake area. Scientific Reports, 7(1): 1–4.

Briere P R. 2000. Playa, playa lake, sabkha: Proposed definitions for old terms. Journal of Arid Environments, 45(1): 1–7.

Buck B J, King J, Etyemezian V. 2011. Effects of salt mineralogy on dust emissions, Salton Sea, California. Soil Science Society of America Journal, 75(5): 1971–1985.

Bullard J E, Harrison S P, Baddock M C, et al. 2020. Preferential dust sources: A geomorphological classification designed for use in global dust-cycle models. Journal of Geophysical Research-Earth Surface, 116: F04034, doi: 10.1029/2011JF002061.

Cahill T A, Gill T E, Reid J S. 1996. Saltating particles, playa crusts and dust aerosols at Owens (dry) lake, California. Earth Surface Processes & Landforms, 21(1): 621–639.

Chico R J. 1968. Encyclopedia of Earth Science. Berlin: Springer Heidelberg, 865–871.

Chun X, Su R, Liu J Y, et al. 2017. Climatic implications on variations of Qehan Lake in the arid regions of Inner Mongolia during the recent five decades. Environmental Monitoring and Assessment, 189(1): 1–11.

Dun H C. 2019. Modeling and simulation of dust emission process in arid and semi-arid regions. MSc Thesis. Lanzhou: Lanzhou University. (in Chinese)

Gill T E. 1996. Eolian sediments generated by anthropogenic disturbance of playas: human impacts on the geomorphic system and geomorphic impacts on the human system. Geomorphology, 17(1–3): 207–228.

Gillett D A. 1979. Environmental Factors Affecting Dust Emission by Wind Erosion. New York: John Wiley & Sons, 71–91.

Goehring L, Conroy R, Akhter A, et al. 2010. Evolution of mud-crack patterns during repeated drying cycles. Soft Matter, 6(15): 3562–3567.

Goehring L. 2013. Evolving fracture patterns: columnar joints, mud cracks and polygonal terrain. Philosophical Transactions of the Royal Society A: Mathematical, Physical and Engineering Sciences, 371(2004): 20120353, doi: 10.1098/rsta.2012.0353.

Goldstein H L, Breit G N, Reynolds R L. 2017. Controls on the chemical composition of saline surface crusts and emitted dust from a wet playa in the Mojave Desert (USA). Journal of Arid Environments, 140: 50–66.

Gomes L, Bergametti G, Coudé-Gaussen G, et al. 1990. Submicron desert dusts: A sandblasting process. Journal of Geophysical Research: Atmospheres, 95(D9): 13927–13935.

Gutiérrez-Elorza M, Desir G, Gutiérrez-Santolalla F, et al. 2005. Origin and evolution of playas and blowouts in the semiarid zone of Tierra de Pinares (Duero Basin, Spain). Geomorphology, 72(1–4): 177–192.

Hahnenberger M, Perry K D. 2015. Chemical comparison of dust and soil from the Sevier Dry Lake, UT, USA. Atmospheric Environment, 113: 90–97.

Hassani A, Azapagic A, Shokri N. 2021. Global predictions of primary soil salinization under changing climate in the 21st century. Nature communications, 12(1): 6663, doi: 10.1038/s41467-021-26907-3.

Houser C A, Nickling W G. 2001. The factors influencing the abrasion efficiency of saltating grains on a clay-crusted playa. Earth Surface Processes & Landforms, 26(5): 491–505.

Huang N, Gu Y D. 2009. Research and development of dust release and sedimentation machine. Advances in Earth Science, 24(11): 1175–1184. (in Chinese)

Krinsley D B. 1970. A Geomorphological and Palaeoclimatological Study of the Playas of Iran: Part I. Prepared for Air Force Cambridge Research Laboratories. Washington, D.C.: Geological Survey, United State Department of the Interior, 277–289.

Krinsley D H, Doornkamp J C. 1973. Atlas of Quartz Sand Surface Textures. In: Cambridge Earth Science Series. Cambridge: Cambridge University Press, 91.

Liu D W, Abuduwaili J, Lei J Q, et al. 2011a. Deposition rate and chemical composition of the aeolian dust from a bare saline playa, Ebinur Lake, Xinjiang, China. Water Air & Soil Pollution, 218(1): 175–184.

Liu D W, Abuduwaili J, Lei J Q, et al. 2011b. Wind erosion of saline playa sediments and its ecological effects in Ebinur Lake, Xinjiang, China. Environmental Earth Sciences, 63(2): 241–250.

Luo H R, Smith L M, Haukos D A, et al. 1999. Sources of recently deposited sediments in playa wetlands. Wetlands, 19(1): 176–181.

Mardi A H, Khaghani A, MacDonald A B, et al. 2018. The Lake Urmia environmental disaster in Iran: A look at aerosol pollution. Science of The Total Environment, 633: 42–49.

Micklin P. 2016. The future Aral Sea: hope and despair. Environmental Earth Sciences, 75(9): 1–15.

Motaghi F A, Hamzehpour H, Mola Ali Abasiyan S, et al. 2020. The wind erodibility in the newly emerged surfaces of Urmia Playa Lake and adjacent agricultural lands and its determining factors. CATENA, 194: 104675, doi: 10.1016/j.catena.2020.104675.

Nield J M, Bryant R G, Wiggs G F S, et al. 2015. The dynamism of salt crust patterns on playas. Geology, 43(1): 31–34.

Nield J M, Neuman C M K, O'Brien P, et al. 2016a. Evaporative sodium salt crust development and its wind tunnel derived transport dynamics under variable climatic conditions. Aeolian Research, 23: 51–62.

Nield J M, Wiggs G, King J, et al. 2016b. Climate-surface-pore-water interactions on a salt crusted playa: implications for crust pattern and surface roughness development measured using terrestrial laser scanning. Earth Surface Processes & Landforms, 41(6): 738–753.

Pagliai M, Stoops G. 2010. Physical and biological surface crusts and seals. In: Interpretation of Micromorphological Features of Soils and Regoliths (2nd ed.). Amsterdam: Elsevier, 419–440.

Peterson F F. 1980. Holocene desert soil formation under sodium salt influence in a playa-margin environment. Quaternary Research, 13(2): 172–186.

Prandtl L. 1935. Aerodynamic Theory. Berlin: Springer Berlin Heidelberg, 34–208.

Reynolds R L, Yount J C, Reheis M, et al. 2007. Dust emission from wet and dry playas in the Mojave Desert, USA. Earth Surface Processes & Landforms, 32(12): 1811–1827.

Schoeneberger P J, Wysocki D A, Benham E C, et al. 2012. Field Book for Describing and Sampling Soils (Version 3.0). Natural Resources Conservation Service, National Soil Survey Center, Lincoln, 75–76.

Stout J E. 2003. Seasonal variations of saltation activity on a high plains saline playa: Yellow Lake, Texas. Physical Geography, 24(1): 61–76.

Stout J E. 2007. Simultaneous observations of the critical aeolian threshold of two surfaces. Geomorphology, 85(1–2): 3–16.

Sweeney M R, McDonald E V, Etyemezian V. 2011. Quantifying dust emissions from desert landforms, eastern Mojave Desert, USA. Geomorphology, 135(1–2): 21–34.

Sweeney M R, Zlotnik V A, Joeckel R M, et al. 2016. Geomorphic and hydrologic controls of dust emissions during drought from Yellow Lake playa, West Texas, USA. Journal of Arid Environments, 133: 37–46.

Tang C, Shi B, Liu C, et al. 2008. Influencing factors of geometrical structure of surface shrinkage cracks in clayey soils. Engineering Geology, 101(3–4): 204–217.

Tao S L, Fang J Y, Zhao X, et al. 2015. Rapid loss of lakes on the Mongolian Plateau. Proceedings of the National Academy of Sciences, 112(7): 2281–2286.

Tran K M, Bui H H, Kodikara J, et al. 2019. Soil curling process and its influencing factors. Canadian Geotechnical Journal, 57(3): 408–422.

Valentin C, Bresson L M. 1992. Morphology, genesis and classification of surface crusts in loamy and sandy soils. Geoderma, 55(3–4): 225–245.

White W H, Hyslop N P, Trzepla K, et al. 2015. Regional transport of a chemically distinctive dust: Gypsum from White Sands, New Mexico (USA). Aeolian Research, 16: 1–10.

Wurtsbaugh W A, Miller C, Null S E, et al. 2017. Decline of the world's saline lakes. Nature Geoscience, 10(11): 816–821.

Xisarula. 2011. Analysis of chagannoor saline-alkaline soil chemical composition and that's effect on biological characteristic of Salsa. MSc Thesis. Huhhot: Inner Mongolia Normal University, 12–13. (in Chinese)

Yechieli Y, Wood W W. 2002. Hydrogeologic processes in saline systems: playas, sabkhas, and saline lakes. Earth-Science Reviews, 58(3–4): 343–365.

Zhang G Q, Yao T D, Chen W F, et al. 2019. Regional differences of lake evolution across China during 1960s–2015 and its natural and anthropogenic causes. Remote Sensing Environment, 221: 386–404.

Zhang J, Shao Y P, Huang N. 2014. Measurements of dust deposition velocity in a wind-tunnel experiment. Atmospheric Chemistry & Physics, 14(17): 8869–8882.

Zhang J, Teng Z J, Huang N, et al. 2016. Surface renewal as a significant mechanism for dust emission. Atmospheric Chemistry & Physics, 16: 15517–15528.

Zhao F, Liu H, Yin Y, et al. 2011. Vegetation succession prevents dry lake beds from becoming dust sources in the semi-arid steppe region of China. Earth Surface Processes & Landforms, 36(7): 864–871.

Zlotnik V A, Ong J B, Lenters J D, et al. 2012. Quantification of salt dust pathways from a groundwater-fed lake: Implications for solute budgets and dust emission rates. Journal of Geophysical Research: Earth Surface, 117: F02014, doi: 10.1029/2011JF002107.

Appendix
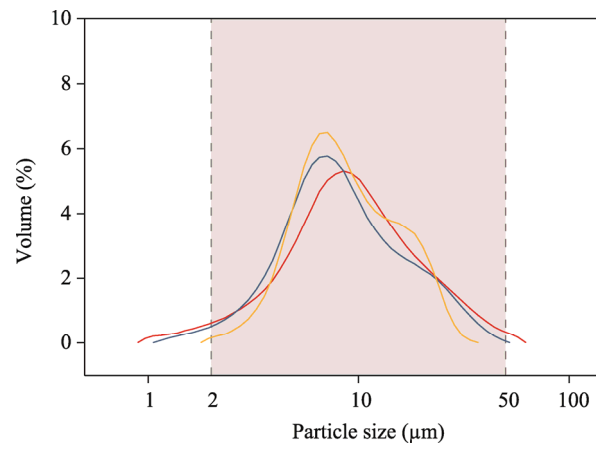
Fig. S1　Particle size distribution of soil samples belonging to clay flats that were not used in the wind tunnel experiments